Available online at www.sciencedirect.com
ScienceDirect
Solid State Sciences 10 (2008) 1864–1874
Solid State Sciences
www.elsevier.com/locate/ssscie

Efficient blue luminescence in Ce^{3+}-activated borates, $A_6MM'(BO_3)_6$

R. Sankar*,[1]

Phosphor Laboratory, Central Electrochemical Research Institute, Karaikudi 630 006, Tamilnadu, India

Received 5 November 2007; received in revised form 1 March 2008; accepted 30 March 2008
Available online 18 April 2008

Abstract

Photoluminescence studies on the Ce^{3+}-activated borates of the type $Sr_6MGa(BO_3)_6$ [A = Sr; M = La, Gd, Lu; M′ = Ga; Ce^{3+} at the M-site], $Sr_6YAl(BO_3)_6$ [A = Sr; M = Y; M′ = Al; Ce^{3+} at the Y-site], $LaSr_5YMg(BO_3)_6$ [A = La, Sr; M = Y; M′ = Mg and Ce^{3+} at the La^{3+}-site] have been carried out for the first time and the results are presented here. All these compounds have been synthesized by the solid state reaction under reducing atmosphere and characterized by powder XRD, TG/DT, density, particle size, SEM, FT-IR and photoluminescence techniques. The photoluminescence of $Sr_6LaGa(BO_3)_6$ activated with low and high Ce^{3+} concentrations has been studied. The luminescence of Ce^{3+} ions substituted at the larger (Gd^{3+}) and smaller (Lu^{3+}) ionic sites have been discussed. Two new compounds $Sr_6CeGa(BO_3)_6$ and $CeSr_5YMg(BO_3)_6$ have also been synthesized and studied. The photoluminescence studies show that under excitation with 254 and 355 nm, all these compounds display efficient blue emission in the region around 400–420 nm. The luminescence properties of these hexaborates under 254 nm excitation are similar to the known blue lamp phosphors $Ca_5(PO_4)_3F:Sb^{3+}$, $Sr_2P_2O_7:Eu^{2+}$, $Sr_5(PO_4)_3Cl:Eu^{2+}$ and the luminescence under 355 nm excitation are similar to the known blue TV phosphor $ZnS:Ag^{+}$. Thus, the borate phosphors can be used as blue components in low pressure mercury vapor (lpmv) lamps and in television tubes.

Keywords: Cerium; Luminescence; Hexaborates

1. Introduction

Phosphors for low pressure mercury vapor (lpmv) lamps, excited by mercury discharge at low pressure corresponding to the radiation of wavelength 254 nm, range from the conventional halophosphate, $Ca_5(PO_4)3F:Sb^{3+}$, Mn^{2+} to the tri-color blend of rare-earth based phosphors. The color rendering index (CRI) of halophosphates are low (∼70) when compared to the tri-phosphors (∼90) [1]. The CRI of halophosphates can be increased without lowering its lumen output of 85 lm/w by adding a broad-band blue emitter to it, which covers the whole of blue region. The phosphor, $Ca_5(PO_4)_3F:Sb^{3+}$ satisfies this requirement. In the case of high efficiency tri-color (trichromatic) fluorescent lamps based on rare-earth phosphors, further improvement of CRI is not a serious requirement. In general, narrow band (or line) emitters help to increase the efficacy while broad-band emitters increase the CRI in lpmv lamps. The main requirements of lpmv phosphors are strong absorption of 254 nm and hence strong emission in the required region when excited with 254 nm. In addition, it must be easily synthesizable, non-toxic, less expensive and stable in air at room as well as high temperatures up to 650 °C. The standard lamp phosphors which meet many of the above requirements are $Ca_5(PO_4)3F:Sb^{3+}$, $BaMgAl_{10}O_{17}:Eu^{2+}$, $Sr_5(PO_4)_3Cl:Eu^{2+}$ and $Sr_2P_2O_7:Eu^{2+}$ [2,3]. Even though these phosphors emit in the required region with high intensity, the phosphates and aluminates require very high processing temperatures (≥1200 °C for phosphates and ≥1500 °C for aluminates). They also require strong reducing atmospheres (H_2 gas flow) to reduce Eu^{3+} to Eu^{2+} at that temperature.

For the color television (CTV), the phosphor ZnS:Ag is the only blue component in use. Here, the phosphor needs to get

* Tel.: +91 9818641828.
E-mail address: ram.sankar@rediffmail.com
[1] Present address: PDP Division, SAMTEL COLOR Limited, Village Chhapraula, Bulandshahar Road, Ghaziabad 201009, UP, India.

1293-2558/$ - see front matter © 2008 Elsevier Masson SAS. All rights reserved.
doi:10.1016/j.solidstatesciences.2008.03.029

excited with long wavelength UV (355 nm) which is compatible with the cathode-ray excitation. For the beam-index phosphor used in television tubes, a short decay time is necessary for the dopant ion so as to avoid afterglow or persistence [2]. The lifetime of an electron in the excited state of Ce^{3+} ion doped in any inorganic crystal lattice is very short. Hence, the Ce^{3+} ion doped lattices are preferred to avoid afterglow. Even though the silicate phosphors, $Y_2Si_2O_7:Ce^{3+}$ (emission at 375 nm) and $Y_2SiO_5:Ce^{3+}$ (blue emission) are known as beam-index phosphors in TV tubes, the silicates not only require high processing temperatures but also require repeated firing and several intermittent grinding at higher temperatures [2].

Hence, our aim is to search for efficient alternatives to the existing blue phosphors for use in lpmv lamps/TV tubes, which can be synthesized at lower temperatures and which are stable in air at room as well as higher temperatures. Our attempts led to the invention of new Ce^{3+}-activated borates of the type $Sr_6MGa(BO_3)_6$ [M = La, Gd, Lu], $Sr_6YAl(BO_3)_6$ and $LaSr_5YMg(BO_3)_6$ [4–6]. Herein we report the synthesis, characterization and photoluminescence of the Ce^{3+}-activated borates. The suitability for application of these borates in lamps and television tubes is checked by comparison with the standard phosphors. The observed results are presented and discussed in the ensuing sections.

2. Experimental details

The samples in polycrystalline form (up to a bulk of 25 g) were synthesized by the conventional high temperature solid state reactions. The starting materials were: RE_2O_3 (RE = La, Gd, Y), CeO_2 all of 99.99% purity (Indian Rare Earths Ltd), Ga_2O_3, Lu_2O_3 (all of 99.99% purity, Cerac), $SrCO_3$ (of 99.5% purity, Lumichem Ltd.), H_3BO_3 (of 99.5% purity, Glaxo (India) Ltd.), MgO (>98% purity, BDH, England) and $Al(NO_3)_3\cdot 9H_2O$ (>98.5% purity, Thomas Baker Ltd.). La_2O_3 was heated in air at 1000 °C for 24 h to remove the moisture and CO_2 present in it and kept in a desiccator. The starting materials were thoroughly homogenized in an agate mortar and then transferred into alumina crucible for heat treatment in a muffle furnace. An excess of 3–5 mol% H_3BO_3 was added to compensate for any loss due to vaporization. An excess of 1 mol% $Al(NO_3)_3\cdot 9H_2O$ was added to compensate for any weight loss. The heat treatment was carried out separately in reducing atmospheres created using N_2:3H_2 gas flow as well as pure H_2 gas flow for about 10–30 h at temperatures ranging from 900 to 1150 °C. All the compounds were cooled inside the furnace to room temperature by furnace shut-off.

Powder X-ray diffractograms (XRD) of the compounds were obtained using a JEOL JDX 8030 powder X-ray diffractometer employing Cu Kα radiation with Ni filter (scan speed 0.1 deg s^{-1}). The observed (*hkl*) reflections were compared with the calculated ones generated using the computer program LAZY PVLVERIX for the different compositions. The crystal data and atom positions were taken from Ref. [5]. The lattice parameters were calculated from the indexed XRD patterns using least-squares refinement (TG/DTA). The thermal analysis measurements (TG/DTA) were carried out in N_2 atmosphere (in the range 25–1000 °C, 10 °C/min) using a simultaneous thermal analysis system (STA 1500; PL Thermal Sci. Ltd., UK). Powder density measurements were calculated using pycnometric technique with xylene as the medium. A 10 ml specific gravity bottle and about 1 g of sample were used for measurement. Particle size analysis was carried out using a MALVERN particle sizer 3600E type (Malvern Instruments, England). The scanning electron micrographs (SEM) of the samples were obtained using a Leica Stereoscan 440 model SEM Instrument fitted with an E5000 polaron coating unit (rating: 10 kV EHT; 25 pA beam current). The samples for SEM were coated with a layer of gold to prevent the charging of the specimen. Fourier transform infra-red spectra of the samples were recorded using a Perkin Elmer Paragon 500 FT-IR spectrophotometer (scan speed: 4 scans in 6 s) with KBr pellet as the reference. The photoluminescence excitation and emission spectra were recorded at room temperature using a Hitachi 650-10S fluorescence spectrophotometer equipped with a 150 W Xenon lamp and a Hamamatsu R928F photomultiplier detector. The integrated emission intensity measurements were carried out for samples taken in equal amounts and prepared under identical conditions. The blue phosphors, viz., $Ca_5(PO_4)_3F:Sb^{3+}$, $CaWO_4$, $ZnS:Ag^+$ and $Sr_5(PO_4)_3Cl:Eu^{3+}$ used for comparison were synthesized in the laboratory. The chemical compositions of these phosphors do not exactly correspond to the materials under investigation. However, we presented the results of the luminescent yield in relation to these known commercial phosphors (relative luminescent yield) because the borate compounds under study appear to have good potential for application.

3. Results and discussion

The compounds are crystalline solids, white in color, stable in air and insoluble in water. The XRD patterns establish the single phase nature of the synthesized compounds and no second phase was noted. The powder XRD details for compound $CeSr_5YMg(BO_3)_6$ [Fig. 1 and Table 1] are shown.

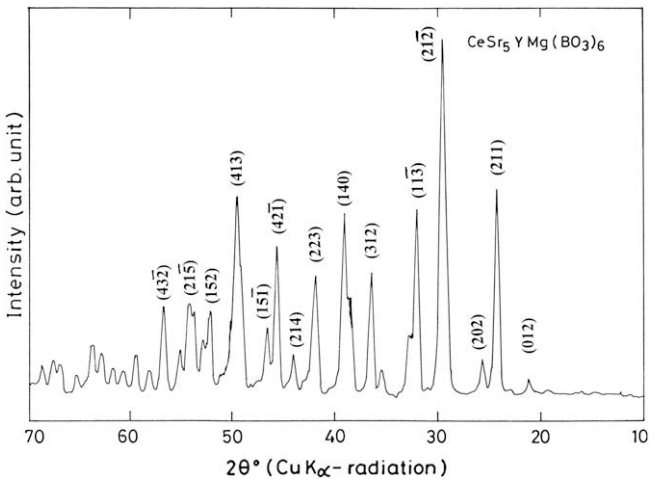

Fig. 1. Powder X-ray diffraction pattern for compound $CeSr_5YMg(BO_3)_6$ [Cu Kα radiation].

Table 1
Powder XRD data of $CeSr_5YMg(BO_3)_6$ compound (Cu Kα radiation)

$2\theta_{exptl}$	$2\theta_{std}$[a]	d_{exptl}	d_{std}[a]	$I/I_{0\ exptl}$	$I/I_{0\ std}$[a]	(hkl)[a]
21.132	21.000	4.204	4.230	7	8	012
24.200	24.170	3.679	3.682	60	64	211
25.626	25.590	3.476	3.481	15	11	202
29.508	29.498	3.027	3.028	100	100	21−2
32.594	32.596	2.747	2.747	23	10	11−3
36.160	36.176	2.484	2.483	40	32	312
38.888	38.814	2.320	2.320	62	20	140
41.618	41.598	2.170	2.171	35	15	223
45.368	45.390	1.999	1.998	45	30	214
46.272	46.272	1.962	1.962	21	7	42−1
48.608	48.692	1.873	1.870	34	22	15−1
49.224	49.224	1.851	1.851	57	17	413
51.828	51.860	1.764	1.763	28	19	152
54.770	54.804	1.676	1.675	29	7	21−5
56.414	56.338	1.631	1.633	40	10	43−2

Rhombohedral−hexagonal system; hexagonal space-group: $R\bar{3}$; least-squares fit lattice parameters: $a = 12.270$ (0.003) Å and $c = 9.220$ (0.004) Å against the values $a = 12.237$ Å and $c = 9.215$ Å for compound $LaSr_5YMg(BO_3)_6$.

[a] Obtained by alternating between the software programs LAZY PULVERIX (a program to generate powder XRD data from single crystal data) and HOCT (a program to calculate the values of lattice parameters from the experimental powder XRD data, by applying the method of least squares).

The least-squares fit hexagonal lattice parameters for $CeSr_5YMg(BO_3)_6$ are $a = 12.270$ (0.003) Å and $c = 9.220$ (0.004) Å against the values $a = 12.237$ Å and $c = 9.215$ Å for compound $LaSr_5YMg(BO_3)_6$ as reported in Ref. [5].

The powder density of compound $Sr_6LaGa(BO_3)_6$ obtained by the pycnometric technique is 4.34 g ml^{-1} against the theoretical value 4.45 g ml^{-1}. The thermal studies on the already formed compounds $Sr_6CeGa(BO_3)_6$ and $CeSr_5YMg(BO_3)_6$ in N_2 atmosphere indicate no phase transition or weight loss in the range 25−1000 °C. The particle size analysis of the $Sr_6CeGa(BO_3)_6$ shows that the particle sizes are in the range 3−27 μm. The SEM studies on compound $CeSr_5YMg(BO_3)_6$ [Fig. 2] show well-defined crystallites of these compounds. The FT-IR spectra recorded for compounds $Sr_6LaGe(BO_3)_6$, $Sr_6CeGa(BO_3)_6$ and $CeSr_5YMg(BO_3)_6$ show the characteristic bands in the range 500−2000 cm^{-1} [Fig. 3] as discussed elsewhere [7].

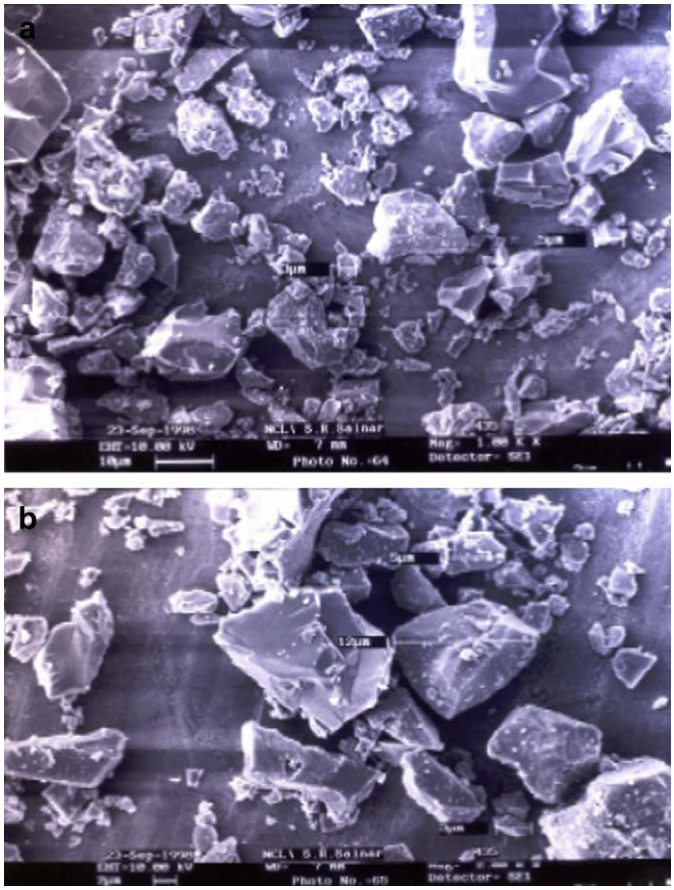

Fig. 2. SEM photographs of compound $CeSr_5YMg(BO_3)_6$ recorded at two different magnifications.

3.1. Ce^{3+} luminescence − general aspects

The efficient luminescence of Ce^{3+} in many inorganic lattices is very well known [8−14]. The ion Ce^{3+} has $4f^1$-electronic configuration. The ground state of Ce^{3+} is the doublet $^2F_{5/2}$ and $^2F_{7/2}$. The lower excited states are the Crystal Field components of the 5d configuration. The Ce^{3+} emission corresponds to transitions from the lowest 5d level to $^2F_{5/2}$ and $^2F_{7/2}$ states of the $4f^1$ configuration. The excited state derived from the 5d state is sensitive to the Crystal Field and is coupled to the lattice vibrations which results in broader band emission rather than line emission. Normally Ce^{3+} emission shows two bands due to the doublet character of the 4f ground state ($^2F_{5/2}$ and $^2F_{7/2}$). The energy difference between $^2F_{5/2}$ and $^2F_{7/2}$ emission doublet is around 2000 cm^{-1}. The absence of the characteristic doublet in any lattice shows that there is a stronger Crystal Field at the Ce^{3+} ions in the lattice and hence leads to extensive splitting of the 4f ground state of Ce^{3+}. The Ce^{3+} emission due to 5d → 4f transition is an allowed electric dipole transition [15]. The occurrence of more than one Ce^{3+} excitation band in any lattice is probably due to the Crystal Field splitting of the 5d (^2D) state. The Ce^{3+} emission will be at lower wavenumbers if the lowest 5d level lies exceptionally low and if the Stokes shift is exceptionally large. The nature of the surrounding ligands also influences the position of the emission bands. The less electronegative ligands shift the emission to longer wavelength due to decrease in 4f−5d energy difference. As the energy levels of Ce^{3+} in crystals are strongly affected by symmetry and Crystal Field of Ce^{3+} in the lattice, optical transitions are known to shift from the UV to visible regions in different host lattices. Increase in Stokes shift results in the broadening of the excitation/emission bands. Thus, the individual excitation (also emission) bands become indistinguishable and appear as single band [16]. The Ce^{3+} emission band can also be broadened by strong electron−phonon coupling or by lattice disorder and hence only single band will appear instead of a doublet due to ground state split [17]. Lesser is the stiffness of the host lattice, larger is the Stokes shift of Ce^{3+}. It is also known that from the ion Gd^{3+} to Lu^{3+}, the optical transitions shift to lower energy, the

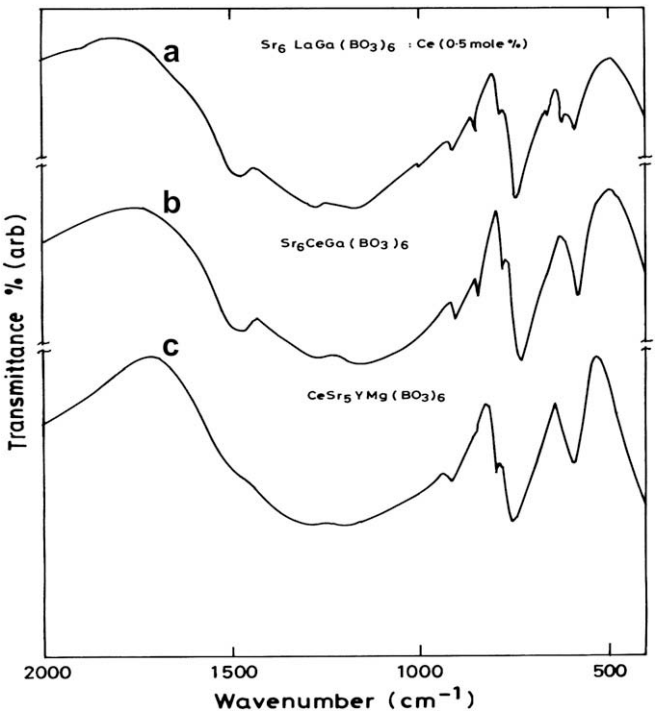

Fig. 3. FT-IR spectra of (a) $Sr_6LaGa(BO_3)_6$:Ce (0.5 mol%), (b) $Sr_6CeGa(BO_3)_6$ and (c) $CeSr_5YMg(BO_3)_6$ recorded in the range 500–2000 cm^{-1}.

Stokes shift increases and the quenching temperature decreases [18].

In any lattice at high Ce^{3+} concentrations, the short wavelength component of Ce^{3+} emission band gets reduced in intensity because of self-absorption [19]. At low Ce^{3+} concentration, the short wavelength emission component dominates and at $x = 1$, the intensity of both the components will be equal. The decrease in intensity of the 5d → $^2F_{5/2}$ 4f component with increase in Ce^{3+} concentration indicates energy migration. Concentration quenching in Ce^{3+}-doped compounds is due to energy migration to impurities or defects. The overlap of excitation and emission bands also leads to concentration quenching. If there is a large spectral overlap, this will result in energy migration between Ce ions in the lattice and also between Ce^{3+} ions in impurities. This will lead to concentration quenching. Quenching can be reduced by a large Ce–Ce interionic distance which reduces the interactions [20]. The higher efficiency at room temperature and the excellent energy migration between Ce^{3+} ions are the two characteristics very much required for Ce^{3+} to be an efficient sensitizer [21].

3.2. $Sr_6LaGa(BO_3)_6:Ce^{3+}$ (at the La-site)

Compound of the form $Sr_6La_{1-x}Ce_xGa(BO_3)_6$ (hereafter referred to as A) where $x = 0.05–1.0$ have been synthesized and their luminescence studied. Even though the luminescence studies have been made on all compositions (for all values of x), only the low ($x = 0.05$) and high ($x = 0.4$) concentrations were taken to facilitate a comparison of the spectra. In compound $Sr_6LaGa(BO_3)_6$:Ce, the Ce^{3+} ion occupies only the La^{3+}-site due to its larger ionic size. Some Ce^{3+} ions may occupy the Sr^{2+}-site also. This is due to the flexibility of the ionic sites and the crystal structure of the borate lattice [5]. The excitation spectrum recorded for compound A with $x = 0.05$ gives a broad excitation band due to the 4f → 5d transition ($^2F_{5/2}$ → 5d level) of Ce^{3+} ion [Fig. 4(a)]. The peak of the excitation band lies around 315 nm. There is a shoulder on this band around 350 nm. This may be due to the 4f → 5d transition ($^2F_{5/2}$ → a different 5d CF level) or may be due to Ce^{3+} ions occupying a different site (Sr^{2+}-site) [22]. The shoulder at 350 nm is of low intensity when compared to the band at 315 nm. The excitation band of Ce^{3+} extends from 245 to 380 nm. Hence, the ion Ce^{3+} can be excited by radiation of wavelengths 254 as well as 355 nm. The excitation band is asymmetrical. When the concentration of Ce^{3+} ions in A is increased to 0.4 i.e., when $x = 0.4$, we get compound $Sr_6La_{0.6}Ce_{0.4}Ga(BO_3)_6$. The excitation spectrum recorded for this compound shows the broad band due to 4f → 5d transition but the shoulder at 350 nm

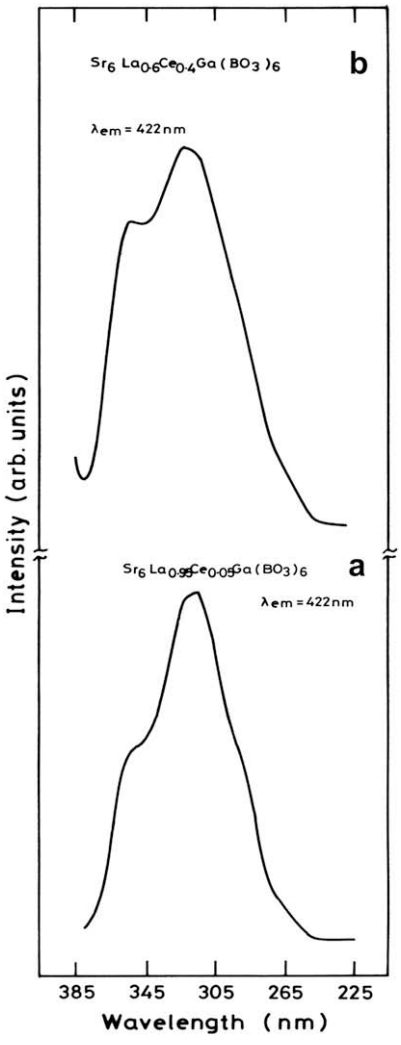

Fig. 4. Excitation spectra of (a) $Sr_6La_{0.95}Ce_{0.05}Ga(BO_3)_6$ and (b) $Sr_6La_{0.6}Ce_{0.4}Ga(BO_3)_6$. $\lambda_{em} = 422$ nm.

increases in intensity [Fig. 4(b)]. All the other spectral features are similar to A with $x = 0.05$.

The emission spectrum recorded for A with $x = 0.05$ under 254 nm excitation gives a broad band extending from 340 to 500 nm and is due to the transition from 5d CF level to the ground state of the Ce^{3+} ion [Fig. 5(a)]. The peak of the emission band lies at 400 nm. The characteristic doublet of Ce^{3+} is not observed in the emission spectrum of A ($x = 0.05$). The Stokes shift of emission is around 6745 cm^{-1}. This is a high value when compared to the value obtained for many of the Ce^{3+}-doped compounds [7,10,12]. It shows that the lattice is less stiff; energy migration is less due to reduction in spectral overlap of excitation–emission bands and hence only a minimum concentration quenching. In addition, it results in broadening of the excitation/emission bands, and also leads to long wavelength emission [14–16,19]. Covalency of the borate also results in larger Stokes shift, as observed in many of these compounds. Because, an increase in covalency between Ce^{3+} and ligand (O^{2-} ion) will result in shifting of 5d level to lower energies (as evidenced here by the excitation which is shifted to longer λ).

The appearance of single emission band in A with $x = 0.05$, without the characteristic doublet, is due to the CF splitting of the ground state, large value of Stokes shift and may also be due to minor disorder of the sites occupied by Ce^{3+} ions in the hexaborate lattice. The emission spectrum recorded for compound A with $x = 0.4$ under 254 nm excitation gives a broad band similar to the one obtained for A with $x = 0.05$ [Fig. 5(b)]. All the spectral features observed are similar to each other.

When the excitation wavelength is changed to 355 nm, the emission spectrum recorded for A with $x = 0.05$ gives a broad band extending from 375 to 470 nm, the peak of which is situated at ~400 nm [Fig. 5(c)]. The band has a shoulder at ~420 nm. The shoulder is nearly equal in intensity to that of the band at 400 nm. The difference in energy between these two bands is around 1200 cm^{-1}, which is less than 2000 cm^{-1}, the theoretical energy difference between the emission doublets. Hence this emission is due to the transition from 5d CF level to the ground states $^2F_{5/2}$ and $^2F_{7/2}$, which is the Ce^{3+} doublet. The Stokes shift amounts to be 6745 cm^{-1}. Hence, under excitation with 355 nm, the characteristic

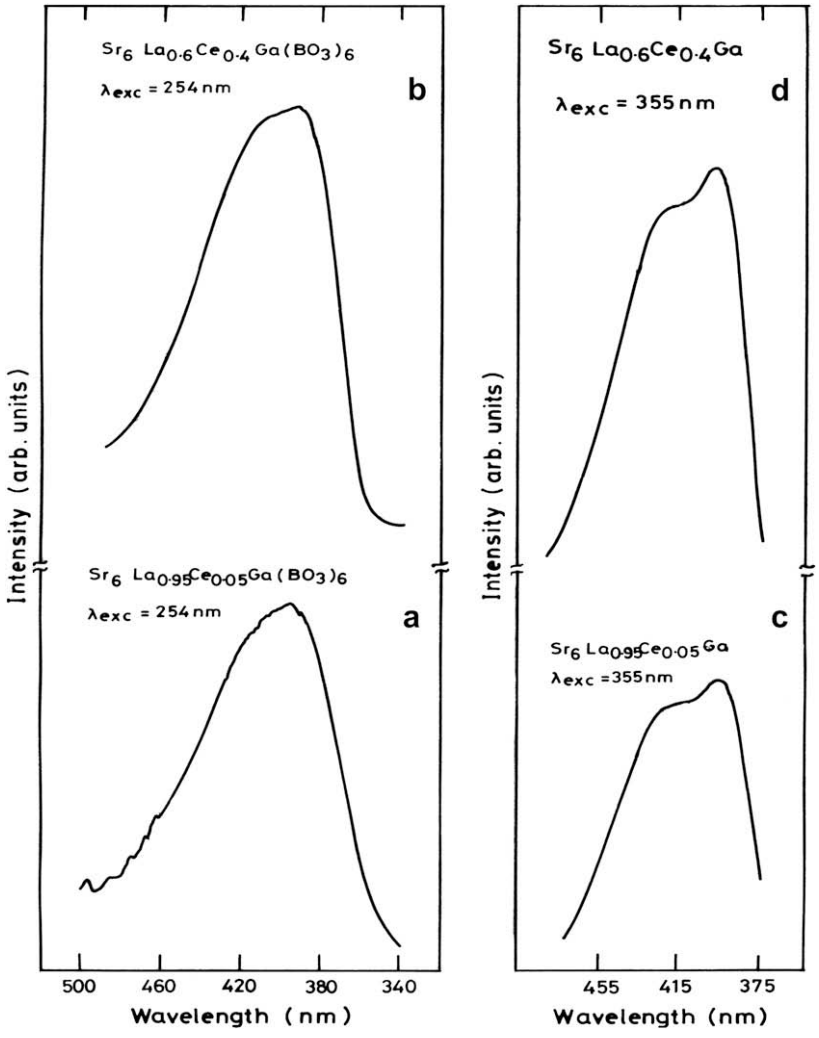

Fig. 5. Emission spectra under 254 nm excitation of (a) $Sr_6La_{0.95}Ce_{0.05}Ga(BO_3)_6$ and (b) $Sr_6La_{0.6}Ce_{0.4}Ga(BO_3)_6$. Emission spectra under 355 nm excitation of (c) $Sr_6La_{0.95}Ce_{0.05}Ga(BO_3)_6$ and (d) $Sr_6La_{0.6}Ce_{0.4}Ga(BO_3)_6$.

emission doublet is observed. The emission spectrum recorded for A with $x = 0.4$ gives similar spectral features to that of A with $x = 0.05$ under 355 nm excitation [Fig. 5(d)].

The excitation spectrum recorded for compound $Sr_6CeGa(BO_3)_6$ ($x = 1$), gives a broad band which peaks at 320 nm with a shoulder at ~350 nm as observed for A with $x = 0.4$ [Fig. 6(a)]. The shoulder at 350 nm increases in intensity and is nearly equal in intensity to that of the band at 320 nm. It is understood that the two components observed in the excitation spectra of A with $x = 0.05$, 0.4 and 1.0 are only due to the transitions from the $^2F_{5/2}$ 4f ground state of Ce^{3+} to the CF levels of the 5d excited state and not from any Ce^{3+} ions occupying an unequivalent site in the lattice. This is clearly evident from Figs. 4 and 6(a) where the excitation spectra were recorded for different emission wavelengths [$\lambda_{em} = 422$ nm for A with $x = 0.5$ and 0.4; $\lambda_{em} = 400$ nm for A with $x = 1.0$]. The change in emission wavelength does not cause any change in the excitation spectra of all these compounds and hence they are found to originate only from similar Ce^{3+}-sites.

It is clearly known that the short wavelength component in the emission spectrum of Ce^{3+} decreases in intensity with increasing Ce^{3+} concentration, the long wavelength component increases in intensity with increasing Ce^{3+} concentration and at $x = 1$, the intensities of both the components will be equal [18]. In compound A with $x = 0.05-1.0$, the long wavelength component increases in emission intensity with increasing Ce^{3+} concentration and at $x = 1$, both the intensities are equal [Figs. 5 and 6(b)]. But it is not clear whether the short wavelength component decreases in emission intensity with increasing Ce^{3+} concentration, in all these compounds. In addition, the Stokes shift is large (>6000 cm^{-1}) which curtails the excitation–emission overlap. Also it is evident from Fig. 7 that the excitation–emission overlap is minimum and hence a minimum energy migration. Hence this clearly guarantees a high intensity emission in all these hexaborates even at high Ce^{3+} concentrations and only a minimum quenching.

The critical distance for energy transfer (R_c) is calculated from the spectral overlap given in Fig. 7. It is known that the value of the critical distance of energy transfer (R_c) in the case of an electric dipole–dipole interaction can be obtained using the formula,

$$R_c^6 = 6.3 \times 10^{27} \frac{4.8 \times 10^{-16}}{E^4} f \times SO$$

where f is the oscillator strength of Ce^{3+}, SO is the spectral overlap in eV and E is the energy at maximum spectral overlap in eV. R_c will be in Angstrom units. The oscillator strength of Ce^{3+} is pre-determined and it amounts to about 5×10^{-8} cm^2 eV. From the spectra given in Fig. 7, it is understood that the values of $\lambda_{overlap}$ and SO are, respectively, $\lambda_{overlap} = 360$ nm and $SO = 53.37 \times 10^2$ eV. The value of E as calculated is $E^{-4} = 7.06 \times 10^{-3}$. Thus the value of $R_c^6 = 57 \times 10^5$. Hence $R_c \approx 13$ Å.

The value of integrated intensities of some of the borates and of the standard blue phosphors under excitation with 254 as well as 355 nm excitation is given in Table 2. It is understood from Table 2 that compound A gives efficient broad-band emission in the blue region similar to the known commercial phosphors and hence is a potential blue phosphor for use in lpmv lamps/television tubes.

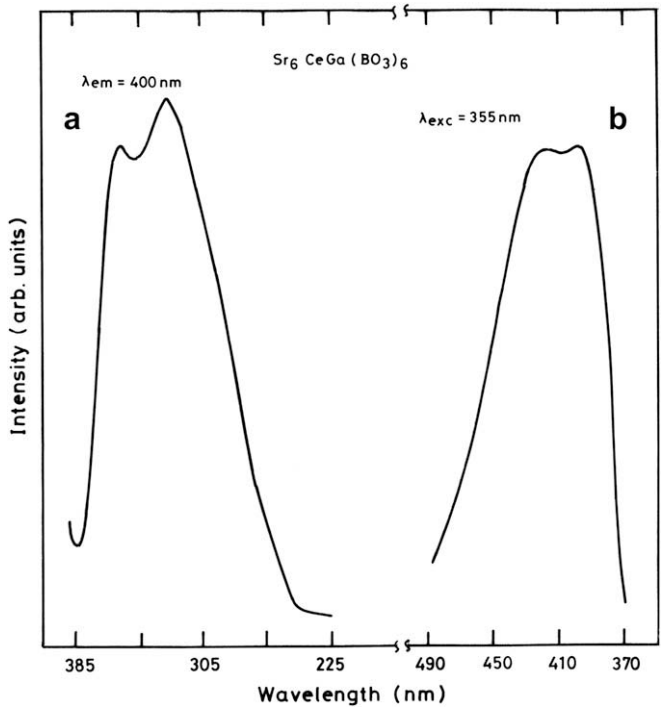

Fig. 6. (a) Excitation and (b) emission spectra of $Sr_6CeGa(BO_3)_6$.

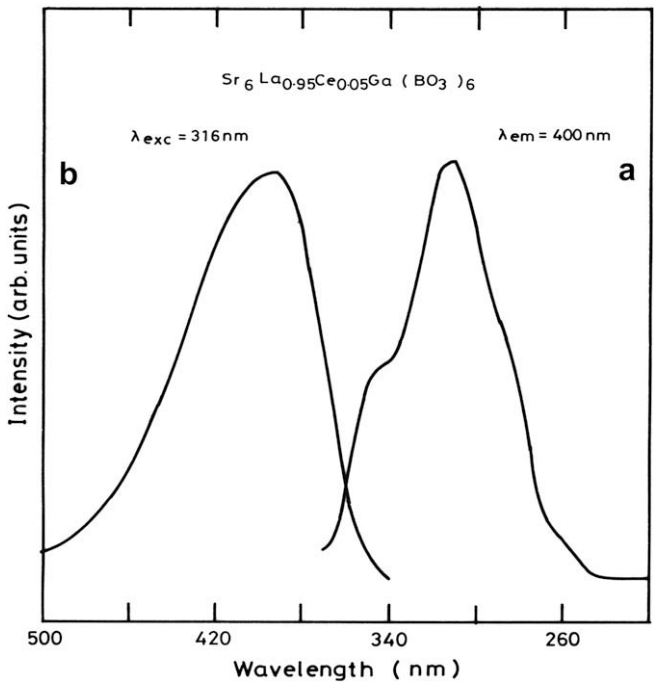

Fig. 7. (a) Excitation and (b) emission spectra of $Sr_6La_{0.95}Ce_{0.05}Ga(BO_3)_6$ showing the spectral overlap.

Table 2
Luminescence properties of the known blue phosphors and the presently studied hexaborates

Compound	Excitation wavelength (nm)	Emission peak (nm)	Nature of emission	Integrated intensity[b] (%)
ZnS:Ag	254	450	Broad band	40
	355	450		85
$CaWO_4$[a]	254	420	Narrow band	50
$Ca_5(PO_4)_3F:Sb^{3+}$, [a]	254	460–480	Broad band	100
$Sr_5(PO_4)_3Cl:Eu^{2+}$	254	450	Narrow band	100
	355	450		100
$Sr_2P_2O_7:Eu^{2+}$	254	420	Narrow band	45
	355	420		91
$Sr_6CeGa(BO_3)_6$	254	400	Broad band	50
	355	400		85
$CeSr_5YMg(BO_3)_6$	254	408	Broad band	50
	355	408		85
$Sr_6Gd_{0.9}Ce_{0.1}(BO_3)_6$	254	400	Broad band	35
	355	400		70
$Sr_6Y_{0.8}Ce_{0.2}$ $Al(BO_3)_6$	254	420	Broad band	45
	355	420		80

[a] The compound cannot be excited with 355 nm.
[b] Even though emission region and spectral shape differ, can be aligned under a common scale, for comparison.

3.3. $Sr_6MGa(BO_3)_6:Ce^{3+}$ $[M^{3+} = Gd, Lu]$

To study the influence of ions of varying ionic radii less than the ionic size of La^{3+} on the luminescence of Ce^{3+}, compounds of the type $Sr_6M_{1-x}Ce_xGa(BO_3)_6$ with M = Gd, Lu have been synthesized and their luminescence studied. Here the ion Gd^{3+} is smaller in size when compared to La^{3+} and the ion Lu^{3+} is the smallest of all (in the lanthanide series). Due to the flexibility of the ionic sites in the hexaborate lattice, the M-site can accommodate ions ranging from La^{3+} to Lu^{3+} [5,7]. As is well known that, the introduction of ions of smaller size will result in a larger Crystal Field at the Ce^{3+} ion-site when compared to the field induced by the La^{3+} ion. As a result, there will be a larger splitting of the Ce^{3+} 5d level which reduces the energy difference between the 4f ground state and the first excited 5d level. This shifts the excitation band towards longer wavelength [10]. The excitation spectrum recorded for compound $Sr_6Gd_{0.99}Ce_{0.01}Ga(BO_3)_6$ (hereafter referred to as B) gives the Ce^{3+} excitation band which is narrow when compared to the excitation band observed for compound A with $x = 0.05$ [Fig. 8(a)]. The peak of this excitation band lies at ~310 nm. The shoulder is observed at ~345 nm, and is not pronounced in intensity. The excitation band extends from 225 to 370 nm. Similar to A, in compound B, the excitation band is asymmetrical. For compound B with $x = 0.1$, the recorded excitation spectra gives similar features to that of B with $x = 0.01$ and no changes are noticed [Fig. 8(b)]. It is clear that the smaller Gd^{3+} environment does not cause any shift in the excitation band towards longer wavelength.

The emission spectrum recorded for compound B with $x = 0.01$ under 254 nm excitation gives a broad band extending from 340 to 500 nm [Fig. 9(a)]. The peak of the band is situated at ~400 nm. The Stokes shift of emission amounts

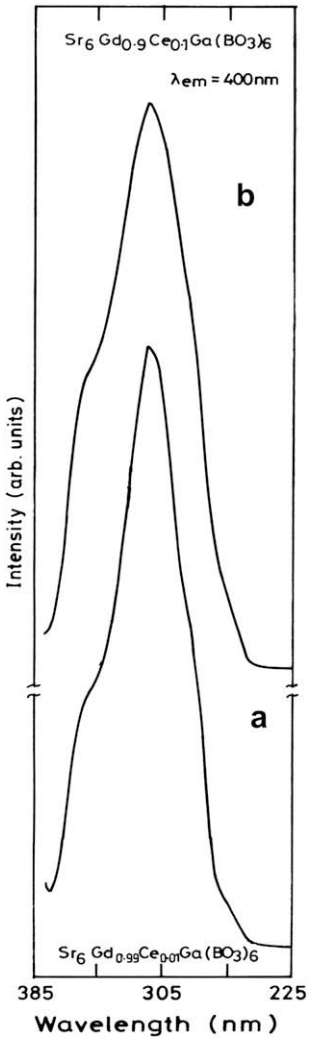

Fig. 8. Excitation spectra of (a) $Sr_6Gd_{0.99}Ce_{0.01}Ga(BO_3)_6$ and (b) $Sr_6Gd_{0.9}Ce_{0.1}Ga(BO_3)_6$. $\lambda_{em} = 400$ nm.

to about 7250 cm^{-1}. The emission spectrum obtained for compound B with $x = 0.1$ under 254 nm excitation is similar to B with $x = 0.01$ without any noticeable change [Fig. 9(b)]. In both the emission spectra, the characteristic doublet is not observed. When excited with 355 nm, compound B with $x = 0.01$ and 0.1 give the emission doublet [Fig. 9(c) and (d)]. The bands cover the region of emission from 375 to 455 nm and the peak of the band is situated at ~400 nm. The long wavelength component is at 420 nm and the energy difference between the doublets is about 1200 cm^{-1}. From the above results, it is clearly understood that the Crystal Field due to the Gd^{3+}-sublattice does not have any noticeable influence on the luminescence of Ce^{3+} ions in compound $Sr_6Gd_{1-x}Ce_xGa(BO_3)_6$. This may be due to the flexibility of ionic sites and the crystal structure of the hexaborate lattice.

For compound $Sr_6Lu_{1-x}Ce_xGa(BO_3)_6$ (hereafter referred to as C) with $x = 0.01$, the recorded excitation spectrum gives an asymmetrical broad band covering the region from 245 to 370 nm [Fig. 10(a)]. The peak of the band is situated at 305 nm and the shoulder on the band is pronounced at

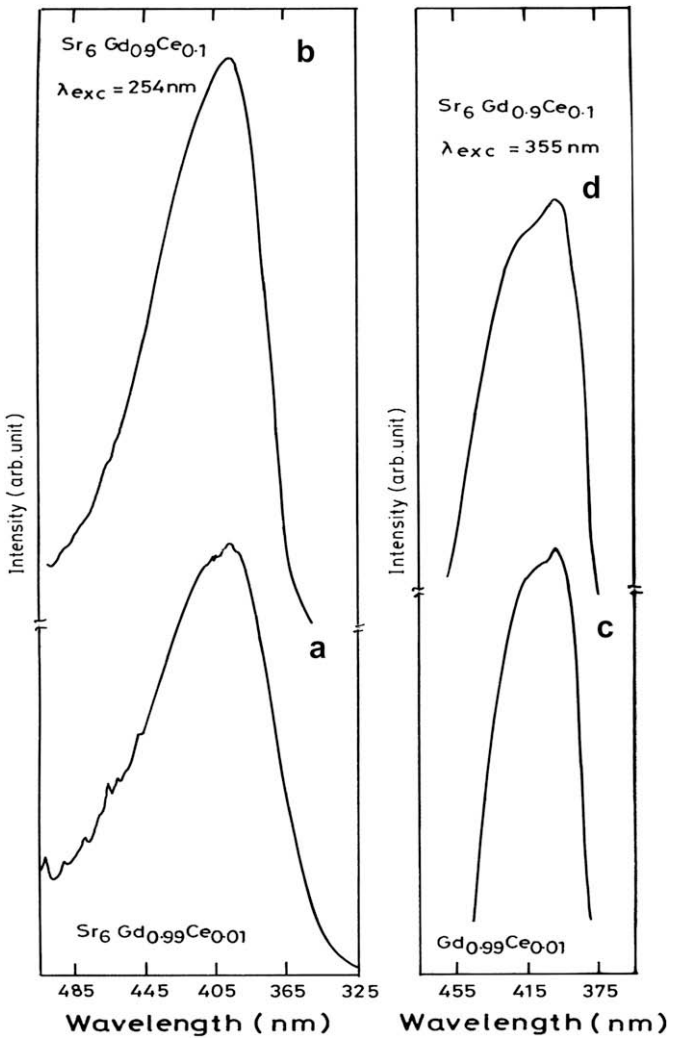

Fig. 9. Emission spectra under 254 nm excitation of (a) $Sr_6Gd_{0.99}Ce_{0.01}Ga(BO_3)_6$ and (b) $Sr_6Gd_{0.9}Ce_{0.1}Ga(BO_3)_6$. Emission spectra under 355 nm excitation of (c) $Sr_6Gd_{0.99}Ce_{0.01}Ga(BO_3)_6$ and (d) $Sr_6Gd_{0.9}Ce_{0.1}Ga(BO_3)_6$.

355 nm. There is one more shoulder observed at 265 nm which may be due to the Ce^{3+} ions occupying a dissimilar site or due to CF splitting of the 5d state. When the Ce^{3+} concentration is increased to 0.1 ($x = 0.1$), the intensity of the long wavelength component increases but the observed spectral features are similar to those of C with $x = 0.01$ [Fig. 10(b)]. The increase in intensity of the long wavelength component with the increase in Ce^{3+} concentration may be due to the excitation–emission overlap or due to energy migration between Ce^{3+} ions. The emission spectra recorded for compound C with $x = 0.01$ and 0.1 under 254 nm excitation give a broad emission band covering the region from 325 to 490 nm without the characteristic doublet [Fig. 10(c) and (d)]. The peak of the band is at ~390 nm. The Stokes shift amounts to about 7146 cm^{-1}. Hence it is understood from the above results that compound C does not have any noticeable influence on the Ce^{3+} luminescence in spite of the smallest Lu^{3+} ionic environment. The Crystal Field of Lu^{3+} ions does not influence the luminescence of Ce^{3+} ions in compound C.

Under excitation with 254 as well as 355 nm, compounds B and C give efficient violet-blue emission. The intensity of emission due to 355 nm excitation is found to have the highest value in all the aforementioned compounds (A–C). The values of integrated emission intensities of B and C are given in Table 2.

3.4. $Sr_6YAl(BO_3)_6:Ce^{3+}$ (at the Y-site)

Since the ions Al^{3+} and Ga^{3+} fall in the same group of the periodic table, compounds of the type $Sr_6Y_{1-x}Ce_xAl(BO_3)_6$ (hereafter referred to as D) ($x = 0.05$–0.3) have been synthesized and their luminescence studied. For $x > 0.3$ (Ce^{3+} content), compound D will not form. The excitation spectrum recorded for compound $Sr_6Y_{0.8}Ce_{0.2}Al(BO_3)_6$ gives a broad, asymmetrical band which peaks at ~315 nm [Fig. 11(a)]. The long wavelength component is not clearly observable and it appears at 345 nm. The region of the band extends from 240 to 385 nm. Hence, this compound can be excited by radiation of wavelengths 254 and 355 nm efficiently. The emission spectrum recorded for compound $Sr_6Y_{0.8}Ce_{0.2}Al(BO_3)_6$ under 350 nm excitation gives a broad band which extends from 370 to 500 nm. The emission band peaks at 420 nm. Contrary to the emission bands observed for compounds A and B under 355 nm excitation, in $Sr_6Y_{0.8}Ce_{0.2}Al(BO_3)_6$, the characteristic doublet is not seen. The absence of characteristic doublet in the emission spectra of Ce^{3+} is due to the extensive CF splitting of the $4f^1$ ground state wherein the levels split by S–O coupling extensively overlap. The Stokes shift of emission amounts to about 7937 cm^{-1}. Hence only a minimum energy migration between Ce^{3+} ions is possible in this lattice.

3.5. $CeSr_5YMg(BO_3)_6$

To study the luminescence of Ce^{3+} ion occupying 9-coordinated A-site, compound of the form $CeSr_5YMg(BO_3)_6$ (hereafter referred to as E) has been synthesized. Here the ion Ce^{3+} prefers to occupy only the 9-coordinated A-site due to the crystal structure of the hexaborate lattice. The excitation spectrum recorded for compound E gives a broad band extending from 240 to 385 nm without any shoulders [Fig. 12(a)]. The peak of the excitation band is at 315 nm. When excited with 254 nm, the obtained emission spectrum gives a broad band extending from 345 to 505 nm, and the peak of this band is situated at 408 nm [Fig. 12(a)]. The characteristic emission doublet is not observed under 254 nm excitation. The Stokes shift amounts to about 7237 cm^{-1}.

3.6. Stokes shift

The Stokes shift of f–d transitions of Eu^{2+} ion in different borates have been nicely discussed based on the crystal structure of compounds by Diaz and Keszler [23]. They have proposed a simple model for the Stokes shift based on the environment of O atoms in the lattice. Accordingly, a large Stokes shift is possible if the O atoms are coordinated by three

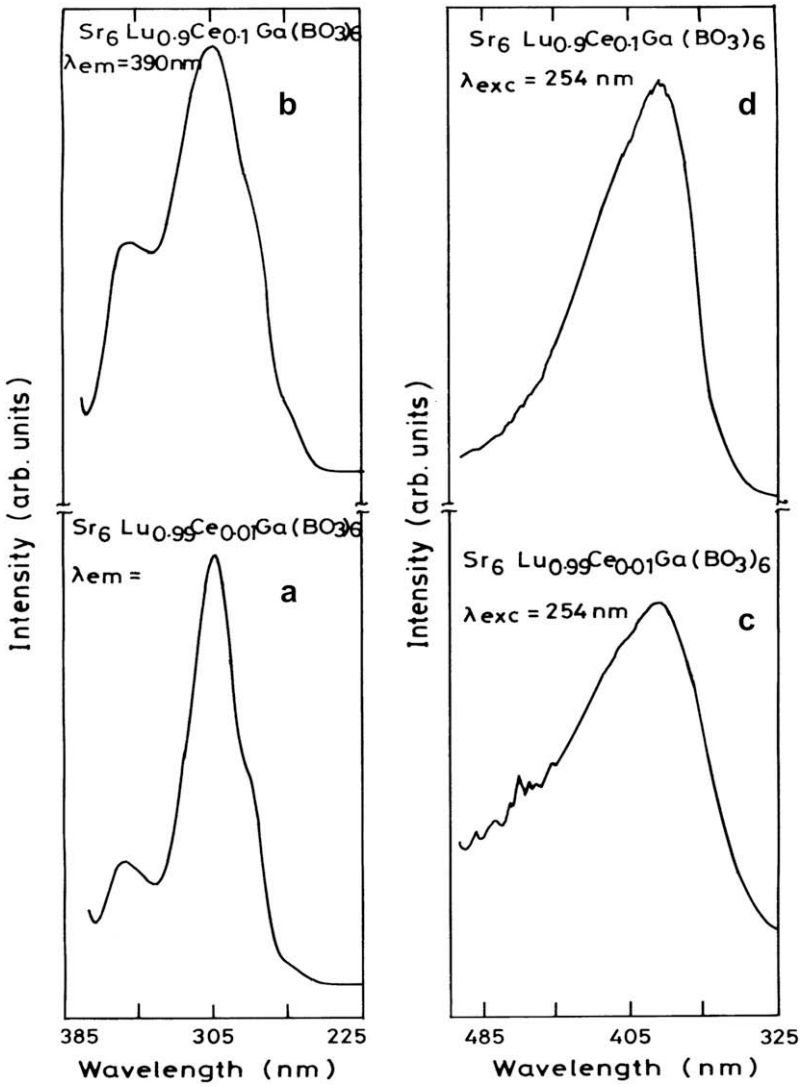

Fig. 10. Excitation spectra of (a) $Sr_6Lu_{0.99}Ce_{0.01}Ga(BO_3)_6$ and (b) $Sr_6Lu_{0.9}Ce_{0.1}Ga(BO_3)_6$. $\lambda_{em} = 390$ nm. Emission spectra of (c) $Sr_6Lu_{0.99}Ce_{0.01}Ga(BO_3)_6$ and (d) $Sr_6Lu_{0.9}Ce_{0.1}Ga(BO_3)_6$. $\lambda_{exc} = 254$ nm.

or more Sr atoms and/or if the O atom polyhedral structure is a distorted one. In the case of O atoms not coordinated by Sr atoms, it is the covalency/nephelauxetic effect which shifts the excitation to longer wavelength resulting in a large Stokes shift. The short wavelength emission will occur for hosts that contain O atoms highly coordinated by B atoms wherein the Stokes shift depends on all the other cations present in the host lattice apart from the dopant site ion.

Table 3 shows the values of Stokes shift of some of the Ce^{3+}-doped borates under study. It is evident that the excitation wavelength lies at a lower energy ($\approx 31{,}000\ cm^{-1}$), the emission is at a higher energy and the Stokes shift is large in all these compounds. Compound $Sr_6CeGa(BO_3)_6$ shows the lowest value of $6250\ cm^{-1}$ and compound $Sr_6Y_{0.8}Ce_{0.2}Al(BO_3)_6$ shows the highest value of $7940\ cm^{-1}$ among the select borates. The comparison between the compounds in Table 3 clearly shows that only the ions present at the M- and M′-sites in the compounds vary except in the case of $CeSr_5YMg(BO_3)_6$ where the ions at the A-site also varies in addition to those present at the M- and M′-sites. All these compounds belong to the same crystal structure and hence no change in the coordination of O atoms with the other atoms (Sr, M, M′ and B atoms) is expected. Also there are only small variations in the angles and interionic distances if we compare those of the individual derivative compounds. The larger ion tends to occupy the M-site with a probability of occupancy close to 89% and the smaller ion tends to occupy the M′-site with a probability of occupancy close to 11%. The interchange of the larger and smaller ions between the M- and M′-sites of the compounds is always possible, but in a limited manner. It is understood from Ref. [5] that each O atom is bonded to more than three Sr atoms in these borates. This clearly shows the reason for large Stokes shift in $CeSr_5YMg(BO_3)_6$ where the dopant Ce^{3+} occupies the Sr position. We also found large Stokes shift values in the case of compounds where the Ce^{3+} occupies only the M-site. It is to be mentioned that the M-site is slightly distorted as evidenced by Eu^{3+} luminescence studies [7] and hence the emission resulting from Ce ion doped at

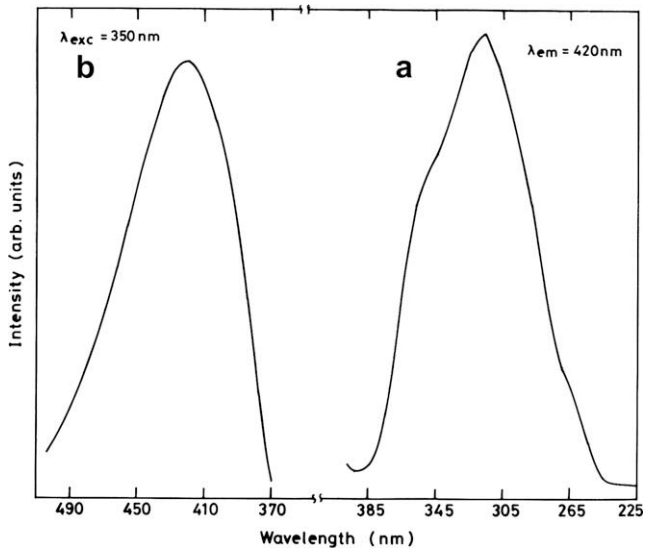

Fig. 11. (a) Excitation and (b) emission spectra of $Sr_6Y_{0.8}Ce_{0.2}Al(BO_3)_6$.

this site is at high energy. Consequently, the covalency/nephelauxetic effect of the borate lattice influences the excitation and shifts it to long wavelengths in all these compounds. Hence the Ce^{3+} ion doped at the M-site gives the long wavelength excitation, short wavelength emission and large Stokes shift as shown in Table 3. The differences observed in the Stokes shift values of the different borate compounds is due to the cations present at the M- and M′-site as per the model proposed by Diaz and Keszler [23].

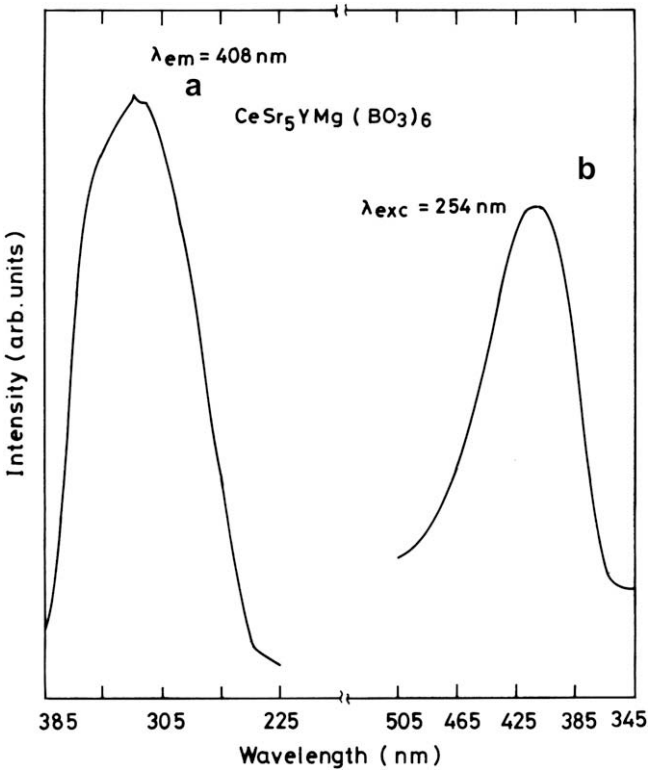

Fig. 12. (a) Excitation and (b) emission spectra of $CeSr_5YMg(BO_3)_6$.

Table 3
Stokes shift values of some Ce^{3+}-doped hexaborates

Compound	λ_{exc} (10^4 cm^{-1})	λ_{em} (10^4 cm^{-1})	Stokes shift (cm^{-1})
$Sr_6La_{0.95}Ce_{0.05}Ga(BO_3)_6$	3.174	2.500	6745
$Sr_6CeGa(BO_3)_6$	3.125	2.500	6250
$Sr_6Gd_{099}Ce_{0.01}Ga(BO_3)_6$	3.225	2.500	7258
$Sr_6Lu_{0.99}Ce_{0.01}Ga(BO_3)_6$	3.278	2.564	7140
$Sr_6Y_{0.8}Ce_{0.2}Al(BO_3)_6$	3.175	2.381	7940
$CeSr_5YMg(BO_3)_6$	3.175	2.451	7240

3.7. Application

It is clearly understood from the luminescence studies on Ce^{3+}-doped hexaborates that these borates can be efficiently excited by light of wavelengths 254 as well as 355 nm. In addition, it is also known that all these borates emit violet-blue color with their emission maxima at ∼400 nm and the emission band covering the region from 345 to 500 nm. It is well known that the excitation by 254 nm radiation is compatible to the excitation inside an lpmv lamp and the excitation by 355 nm is compatible to cathode-ray excitation applied in televisions. Thus, these borates can be applied as broad-band violet-blue phosphors in lpmv lamps and in television tubes. In addition, these borates can also be used to improve the CRI of deluxe lpmv lamps due to their broad band (also high intense) emission. The luminescence properties of the standard blue phosphors and the Ce^{3+}-doped hexaborates are given in Table 2 to highlight the application potential of the hexaborates.

3.8. Advantages [24]

1. The Ce^{3+}-doped hexaborates can be easily synthesized at lower temperatures (≤1000 °C) under mild reducing atmospheres when compared to many of the commercial blue phosphors.
2. The Ce^{3+}-doped borates can be excited directly with radiation of wavelengths 254 as well as 355 nm. No afterglow or persistence of emission observed in the Ce^{3+}-doped hexaborates.
3. These borates are stable in air when heated at room and at higher temperatures (≤650 °C).
4. The hexaborates require only less expensive raw materials for the synthesis.
5. The hexaborate phosphors are stable even when subjected to several hours of ball-milling and are stable to dispersion in aqueous solutions.

4. Conclusions

The photoluminescence studies on the Ce^{3+}-activated hexaborates, $A_6MM'(BO_3)_6$ led to the invention of several new blue phosphors. All these phosphors are synthesized by high temperature solid state reaction under mild reducing atmosphere and characterized by powder XRD, TG/DT, density, particle size, SEM, FT-IR and PL techniques. The polycrystalline borates show high density, narrow particle size

distribution, excellent morphology and no phase transition. The photoluminescence excitation and emission spectra reveal the high intense blue emission of the hexaborates under excitation with light of wavelengths 254 and 355 nm. The spectral properties of the hexaborates are compared with the standard blue phosphors applied in lamps and in television tubes. The hexaborates have several advantages like low temperature synthesis, stability in air at room/high temperatures, less expensive raw materials and no afterglow emission. Because of all these qualities, the hexaborates can be used as efficient blue components in lamps and in television tubes.

Acknowledgements

I am grateful to Prof. G.V. Subba Rao for leaving this paper generously to me to publish as single author.

Acknowledgements are also due to Dr. A. Mani for XRD studies, Dr. V. Sundaram for thermal studies (TG/DT), Mr. L.K. Srinivasan for particle size analysis technique, Dr. Sainkar, NCL-Pune for SEM studies, Mr. A. Muthukumaran for FT-IR studies, Mr. N. Ramakrishnan for typing the manuscript and Mr. S.P. Pandurangan for the drawings.

References

[1] B.M.J. Smets, Mater. Chem. Phys. 16 (1987) 283.
[2] G. Blasse, E.C. Grabmaier, Luminescent Materials, Springer-Verlag, Berlin, 1994.
[3] T. Justel, H. Nikiol, C. Ronda, Angew. Chem. Int. Ed. 37 (1998) 3084.
[4] K.I. Schaffers, T. Alekel III, P.D. Thompson, J.R. Cox, D.A. Keszler, J. Am. Chem. Soc. 112 (1990) 7068.
[5] K.I. Schaffers, T. Alekel III, P.D. Thompson, J.R. Cox, D.A. Keszler, Chem. Mater. 6 (1994) 2014.
[6] P.D. Thompson, D.A. Keszler, Chem. Mater. 6 (1994) 2005.
[7] R. Sankar, G.V. Subba Rao, J. Alloys Compd. 281 (1998) 126.
[8] Xiaohua Liu, Shaojun Chen, Xiaodong Wang, Chem. Phys. Lett. 445 (2007) 32.
[9] R. Ternane, M.T. Cohen-Adad, G. Panczer, C. Goutaudier, C. Dujardin, G. Boulon, N. K-Ariguib, M. T-Ayedi, Solid State Sci. 4 (2002) 53.
[10] B. Saubat, C. Fouassier, P. Hagenmuller, Mater. Res. Bull. 16 (1981) 193.
[11] H.S. Kiliaan, J.F.A.K. Kotte, G. Blasse, J. Electrochem. Soc. 134 (1987) 2359.
[12] Y.Q. Li, G. de With, H.T. Hintzen, J. Lumin. 116 (2006) 107.
[13] R. Le Toquin, A.K. Cheetham, Chem. Phys. Lett. 423 (2006) 352.
[14] V. Dotsenko, J. Mater. Chem. 10 (2000) 561.
[15] G. Blasse, A. Bril, J. Chem. Phys. 47 (1967) 5139.
[16] M.J. Knitel, P. Dorenbos, C.M. Combes, J. Andriessen, C.W.E. van Eijk, J. Lumin. 69 (1996) 325.
[17] M. Yamaga, T. Imai, N. Kodama, J. Lumin. 87–89 (2000) 992.
[18] W.J. Schipper, G. Blasse, J. Alloys Compd. 203 (1994) 267.
[19] Shi-Jin Ding, D.W. Zhang, P.F. Wang, Ji-Tao Wang, Mater. Chem. Phys. 68 (2001) 98.
[20] J.M.P.J. Verstegen, J.L. Sommerdijk, J.G. Verriet, J. Lumin. 6 (1973) 425.
[21] Li You Mo, F. Guillen, C. Fouassier, P. Hagenmuller, J. Electrochem. Soc. 132 (1985) 717.
[22] H.S. Kiliaan, P. van Herwijnen, G. Blasse, J. Solid State Chem. 74 (1988) 39.
[23] A. Diaz, D.A. Keszler, Chem. Mater. 9 (1997) 2071.
[24] G.V. Subba Rao, R. Sankar, US Patent 6165385, 2000.